

SIMULTANEOUS MEASUREMENT OF MULTIPLE CAPILLARY PRESSURE CURVES FROM WETTABILITY AND ROCK PROPERTY VARIATIONS WITHIN SINGLE ROCK PLUGS

E. A. Spinler¹, B. A. Baldwin¹ and A. Graue²
¹Phillips Petroleum Co., Bartlesville OK, USA
²University of Bergen, Norway

Abstract

The high definition capability of Magnetic Resonance Imaging (MRI) makes it suitable for imaging fluids in porous rock on a fraction of a millimeter scale. Under the right circumstances, MRI images of heterogeneous rock containing fluids can become an asset for obtaining data. By using MRI, it was possible to obtain multiple capillary pressure curves simultaneously from core plugs containing immiscible fluids. One example shows how independent and distinct primary drainage capillary pressure curves were obtained for each rock type within a single plug. Another example using the Direct Measurement of Saturation Method for capillary pressure found multiple spontaneous and forced imbibition capillary pressure curves within a single plug that had been aged under crude oil for wettability alteration. Amott indices calculated from these Direct Measured imbibition curves indicated that wettability varied from moderately to highly water-wet conditions within the plug with the least water-wet rock toward the outside of the plug. The variation of wettability within the plug could not be discerned from an Amott test on the full plug. Analysis of such wettability variations within a single plug was only possible by the Direct Measurement of Saturation Method.

Introduction

Application of laboratory data from core analysis to reservoir studies can be seriously handicapped by the quality of data. Non-uniformity in the properties of rock samples is often a major source of poor quality information. When cored material is naturally too heterogeneous for studies or too expensive to obtain, outcrop rock is usually substituted. Imaging technology can aid in screening core and outcrop for variations of pore structure such as porosity and lithology. Both core material and outcrop rock must frequently be properly conditioned in the laboratory to be useable. This may require aging in crude oil or other means to attain the desired wettability. With the current technology, the wettability state of a rock sample can be measured by a number of means that are assumed to provide an average wettability for the sample. Wettability variations in rock can occur, however, they can not be seen except on a pore level¹. Such variations can have as much if not more impact than rock structure on fundamental laboratory measurements like relative permeability and capillary pressure curves.

This paper will illustrate some of the techniques that were used to obtain quality data from heterogeneous rock. MRI has sufficient definition to evaluate porous rock on less than a millimeter scale. Imaging of the fluids in a porous rock provided an enhanced means of obtaining saturation profiles that were used with pressure information to obtain capillary pressure curves. A methodology for Direct Measurement of Saturation Method for capillary pressure (Pc) curves from MRI of fluid saturation profiles as generated by centrifuge was previously presented in the literature^{2,3,4}. The direct measurement of saturation method can reduce or eliminate many of the major limitations of other capillary pressure methods. Most other methods can take a considerable length of time to obtain data, require a model to estimate the proper shape of Pc curves, can not easily obtain positive imbibition Pc data, do not readily recognize rock heterogeneity, etc. This paper will focus on rock heterogeneity in both porosity and wettability that was first recognized and subsequently turned into an asset for obtaining additional capillary pressure data.

Equipment, Materials and Methods

The rock samples were low permeability chalk and the saturating fluids were air and either n-decane or octadecane as a non-wetting fluid with water as the wetting fluid. Both the n-decane and octadecane had a stated purity of 99%+.

Centrifuges with swinging buckets were used to develop saturation profiles in the rock plugs. Heating and cooling was employed as needed to melt or solidify the octadecane.

Saturation measurements were determined from MRI. Images were obtained with a Varian 85/310 CSI. It has a 31 cm bore, 2T superconducting magnet and operates at 85.55 Mhz for hydrogen protons. A 9 cm I.D. saddle coil was used as both transmitting and receiving coil. The amount of fluid hydrogen protons was obtained using the Hahn spin-echo sequence with a 4 ms echo time and a 2.0 second recovery time. One slice, approximately 4 mm thick, was obtained through the center axis of the plug. This orientation produces a rectangle which shows the saturation gradient aligned parallel to the centrifugal axis. The field of view was 9 cm x 8 cm with a pixel resolution of 0.52 x 0.62 mm. 16 repetitive measurements were averaged at each data point. The images consist of 255 levels of gray in a 256 x 256 display. The intensity of the individual pictures were adjusted to produce a presentable visual display, however, for quantitative determinations absolute intensities were used.

Results and Discussion

Plug A was a chalk plug with 25.5 % porosity. When desaturated step-wise with air, using a centrifuge, from 100% brine saturation, distinct bands that represented zones of varying porosity were observed within the plug (see Figures 1 to 4). Higher amounts of water as imaged by MRI were represented by lighter intensities. Air does not image with MRI and resulted in darkening within the plug. Initially at 100% brine saturation (Figure 1), slightly brighter bands represented areas containing additional water, hence higher porosity. The calculated porosity varied from 23 to 27%. To observe the desaturation process, the plug was centrifuged under air (as the non-wetting phase) for varying lengths of time and various speeds (Figures 2 to 4). The angular band-wise development of the saturation profile indicated that the higher porosity areas of the plug desaturated more easily (as represented by the darker areas containing less brine and more air). Without imaging, the non-uniformity of the plug would not have been known and data such as a primary drainage capillary pressure curve would have been compromised by using conventional techniques. By knowing that areas of different porosity existed, it was possible to separately evaluate the desaturation of the different porosity areas. This was done using the 100% brine saturated image (Figure 1) as a guide to selection of areas in the equilibrium image (Figure 4). Intensities of these areas were measured, converted to water saturation and plotted versus pressure as calculated from the standard centrifuge equation as a function of position within the plug. The results of these measurements were two distinct primary drainage capillary pressure curves (Figure 5). The upper most curve represented the lower porosity areas of the plug and the lower curve represented the higher porosity areas.

Plug B was a Portland chalk outcrop plug with 48% porosity (designated plug CHP 4 in reference 5). Its wettability was altered by aging at elevated temperature under crude oil until it appeared to be nearly neutral wet (Amott Water Displacement Index⁶ = 0.07) based on a subsequent imbibition test (Figure 6) and forced water-flood displacement. To obtain capillary pressure curves by using the Direct Measurement of Saturation Method, the imbibition oil, n-decane, was replaced by flowing octadecane at 35°Celsius through the plug. Octadecane has a melting point of 27°Celsius and, when solid, was used to fix the spatial position of fluids within the plug. Since as a solid, octadecane does not image by MRI, imaging of the plug at laboratory conditions of 23°Celsius made it possible to obtain the water saturation distribution directly from the image intensities.

Starting at an average initial water saturation in the plug of 25% (Figure 7), plug B was centrifuged under brine and octadecane at 35°Celsius until capillary equilibrium was reached (14 days). Prior to the MRI measurement, the plug was cooled while at speed in the centrifuge to solidify the octadecane. The resultant image (Figure 8) displayed the fluid distribution for spontaneous and forced imbibition in the plug. There were no artifacts of the centrifugal field in the image because it represented only a 4 millimeter thick slice that was orientated parallel to the centrifuge axis. A fracture is visible in the image slightly to the left of center. This fracture occurred during the centrifuging, but did not impede the analysis. The brightest areas outside of the plug represented free water and its uppermost edge was the free water level or the boundary with the octadecane. The free water level was also observed in the fracture. A most unusual feature of the fluid distribution was the apparent concave downward shape of the saturation distributions within the plug from side edge to side edge. This feature suggested that the properties within the plug varied from the interior to the edges. To evaluate this anomaly required that each column of pixels

making up the image be evaluated separately. Spontaneous and forced imbibition capillary pressure curves were determined for different positions within the plug as indicated by the vertical lines on the shaded contour map of Figure 8 and assigned a 2 letter description for tracking. The capillary pressure by definition was zero at the free water level. These capillary pressure curves (Figures 9a to 14a) showed that the apparent wettability of the plug varied from strongly water-wet at the center to moderately water wet near the edges (Figure 15). The capillary pressure curves were truncated at their tops and bottoms to examine only the influence of varying wettability perpendicular to the plug axis. Wettabilities were calculated from the water saturation at the $P_c=0$ crossing for the spontaneous imbibition endpoint and from the water saturation for the vertical portion of the negative capillary pressure curve. The different shapes to the capillary pressure curves were consistent with the calculated wettabilities with more water-wet rock having higher capillary pressures at any particular water saturation and higher residual oil saturation for the greater negative capillary pressures.

The possible influence of porosity and initial water saturation on the capillary pressure curves was also examined. The porosity variation within the plug was obtained from an image of the plug saturated 100% with n-decane (Figure 16). Image intensity was used to obtain values of porosity for each pixel position within the plug image. Brighter intensity meant more n-decane at that location within the plug and consequently more porosity; zero intensity meant no porosity. The porosity was calculated by assuming that the average intensity for the plug image was equal to the measured plug porosity. The left side of plug image contained calculated porosity generally greater than 50% and the right side of the plug image contained porosity of generally 50% or less. The porosity and initial water saturation for the same pixel positions (Figures 9b to 14b) were observed to have only minor effects on the respective capillary pressure curves. This may be due to porosity and initial water saturation variations affecting the capillary pressure saturation in opposing directions. No further examination of these parameters was conducted.

The variation of wettability within the plug was probably a result of the core preparation process. The plug had been aged in crude oil after it had been flushed to initial water saturation with crude oil. The soaking process in crude oil probably altered the outside of the plug to a neutral or oil-wet state while only altering the interior to the extent that the polar or other components of the crude diffused into the plug. Further core preparation details are present in the references. This would account for both the observed imbibition and the capillary pressure results. A measure of the intensities for such a confirmation of the water saturation profile for capillary pressure close to the side edges of the plug image was not obtainable. The MRI software transform and the high signal contrast between the plug interior and the free water intensity compromised the measured intensities near the edges.

Both of the above examples illustrate the proficiency of Direct Measurement of Saturation for capillary pressure measurement. No other technology can obtain such data from highly heterogeneous rock samples. The recognition of wettability variations caused by rock preparation may be a cause for concern for those who use similar aging methods. The ability to obtain positive capillary imbibition curves for tight rocks such as chalk will impact our understanding and numerical modeling of fluid flow in such media and will certainly better define the Improved Oil Recovery opportunities available.

Conclusions

- 1) Direct Measurement of Saturation for capillary pressure can provide usable, quality data from heterogeneous rock samples. This capability is unique to this methodology.
- 2) Heterogeneity from wettability variations on a millimeter scale in rock samples was recognized and quantified.
- 3) Complete imbibition capillary pressure curves with both spontaneous and forced components provide an accurate measure of wettability.
- 4) Some methodologies for preparing rock plugs may introduce undesired wettability variations that are not discernable by displacement measures of wettability.

Acknowledgements

The authors thank Phillips Petroleum Company for permission to publish this paper. Thanks are given to R. King, J. Stevens, K. Farmer and D. Chancellor for their assistance in the laboratory.

References

1. Rassi-Rihri, O., Robin, M., Rosenberg, E., "Wettability Studies at the Pore Level: A New Approach by the Use of Cryo-Scanning Electron Microscopy", *66th Annual Tech. Conf. and Exhib. of SPE.* (1991) SPE paper 22596.
2. Baldwin, B. A. and Spinler, E. A., "A Direct Method for Simultaneously Determining Positive and Negative Capillary Pressure Curves in Reservoir Rock", *Journal of Petroleum Science and Engineering* (1998) **20**, 161-165.
3. Spinler, E. A. and Baldwin, B. A., "A Direct Method for Determining Complete Positive and Negative Capillary Pressure Curves for Reservoir Rock using the Centrifuge", *4th International Reservoir Characterization Technical Conference proceedings.* (1997)
4. Spinler, E. A. and Baldwin, B. A., "Capillary Pressure Scanning Curves by Direct Measurement of Saturation", *1997 International Symposium of the Society of Core Analysts.* (1997) SCA paper 9705.
5. Graue, A., Bognoe, T., Moe, R., Baldwin, B. A., Spinler, E. A., Maloney, D., "Impacts of Wettability on Capillary Pressure and Relative Permeability", *1999 International Symposium of the Society of Core Analysts.* (1999) SCA paper 9907.
6. Amott, E., "Observations Relating to the Wettability of Porous Rock", *Trans., AIME* (1959) **216**, 156-162.

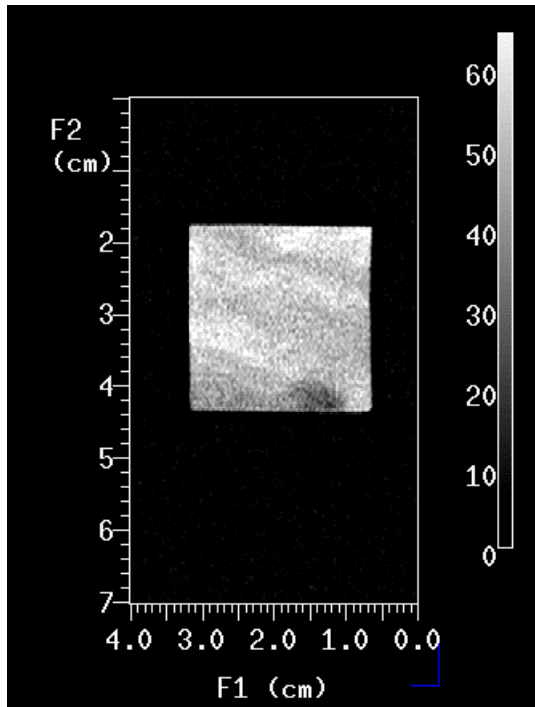


Figure 1 Plug A saturated with 100% brine. The grayer zones are areas of less porosity.

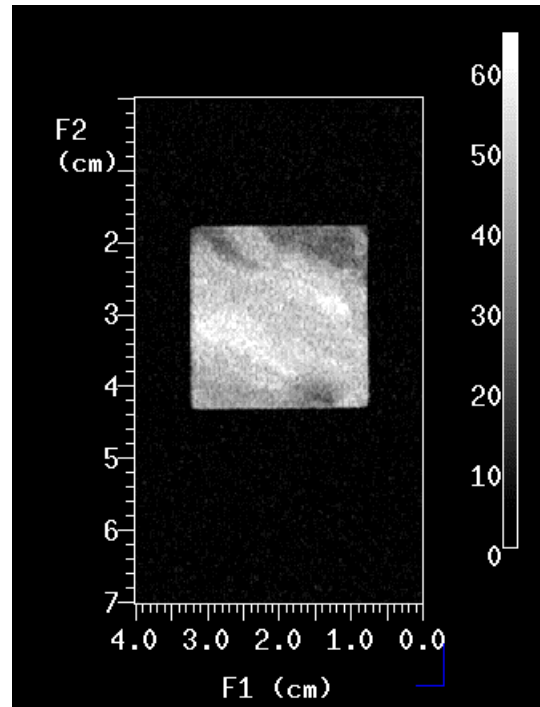


Figure 2 Plug A partially desaturated with air seen as the darker streaks in zones of higher porosity.

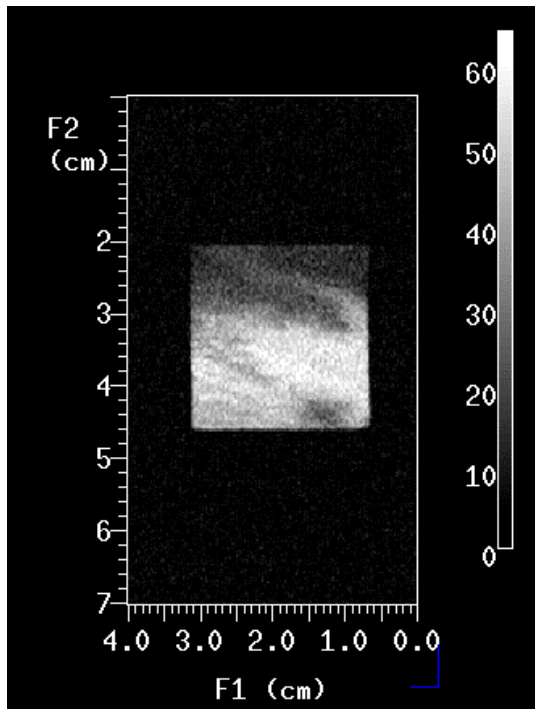


Figure 3 Plug A showing desaturation with air continuing preferentially in the higher porosity areas.

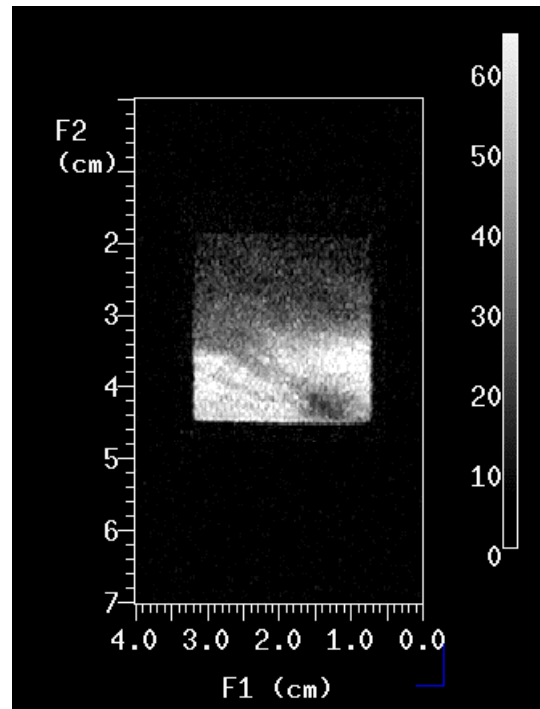


Figure 4 Plug A at an equilibrium desaturated state with air.

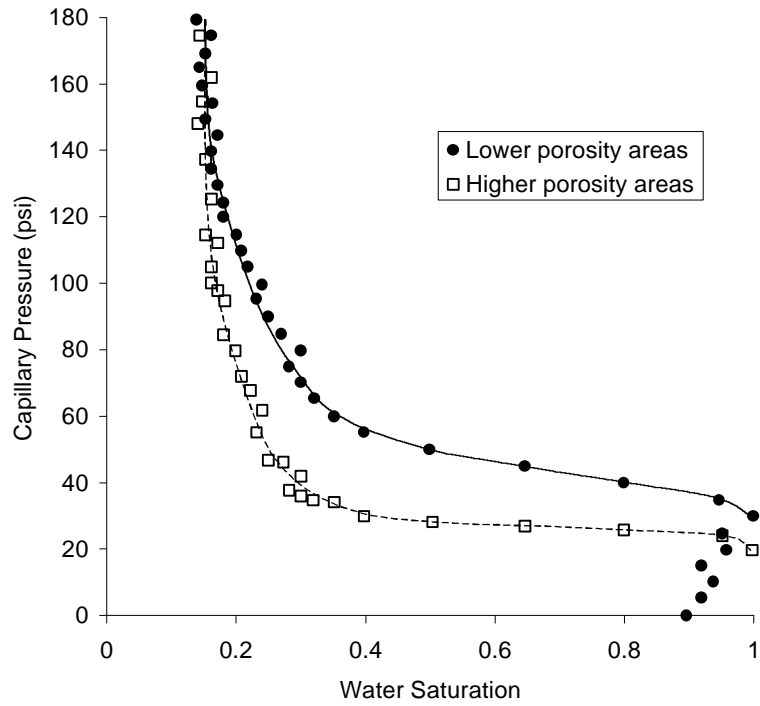


Figure 5 Primary drainage capillary pressure curves at equilibrium for air-brine from manual readings of saturation data from different porosity areas of Plug A.

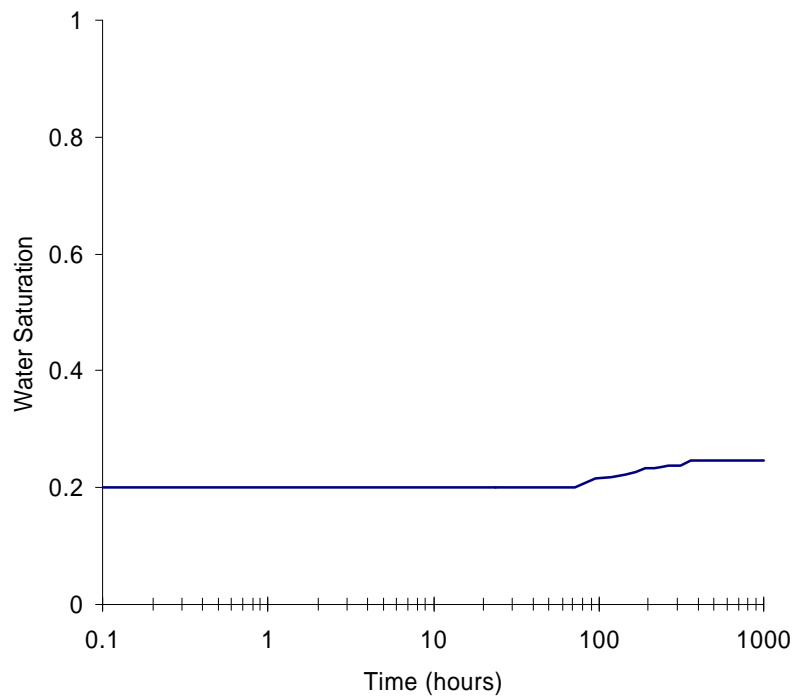
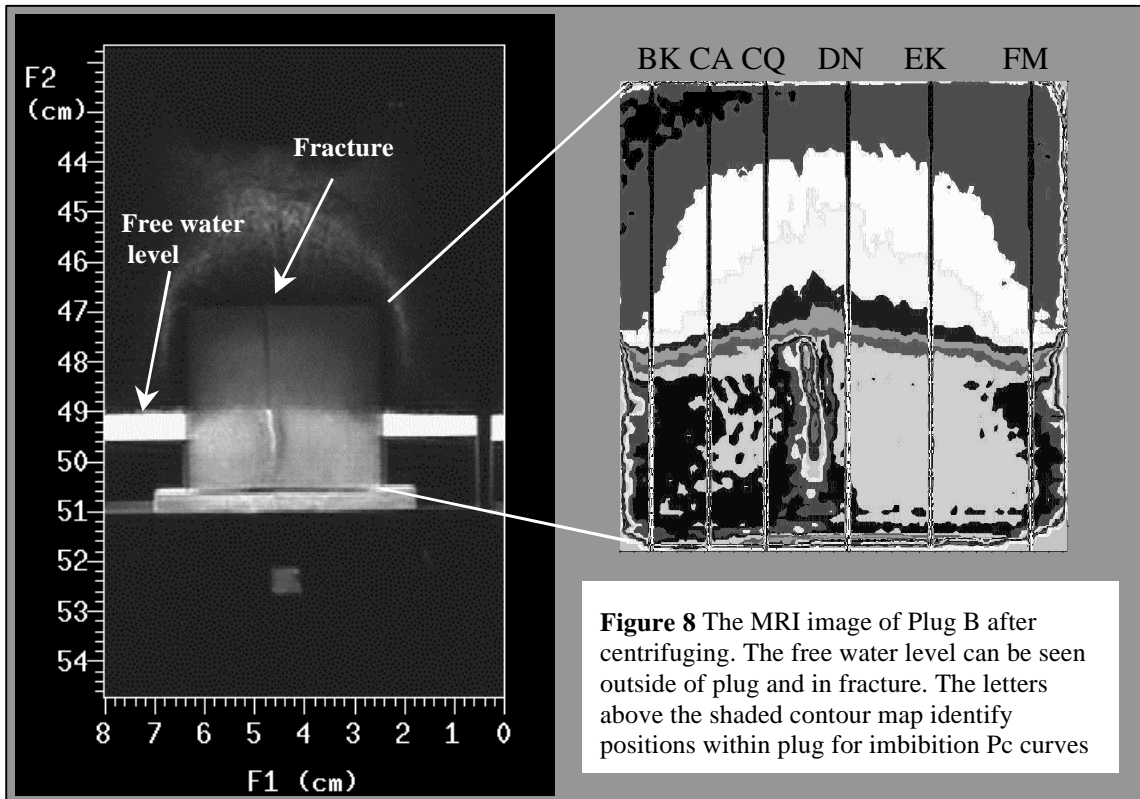
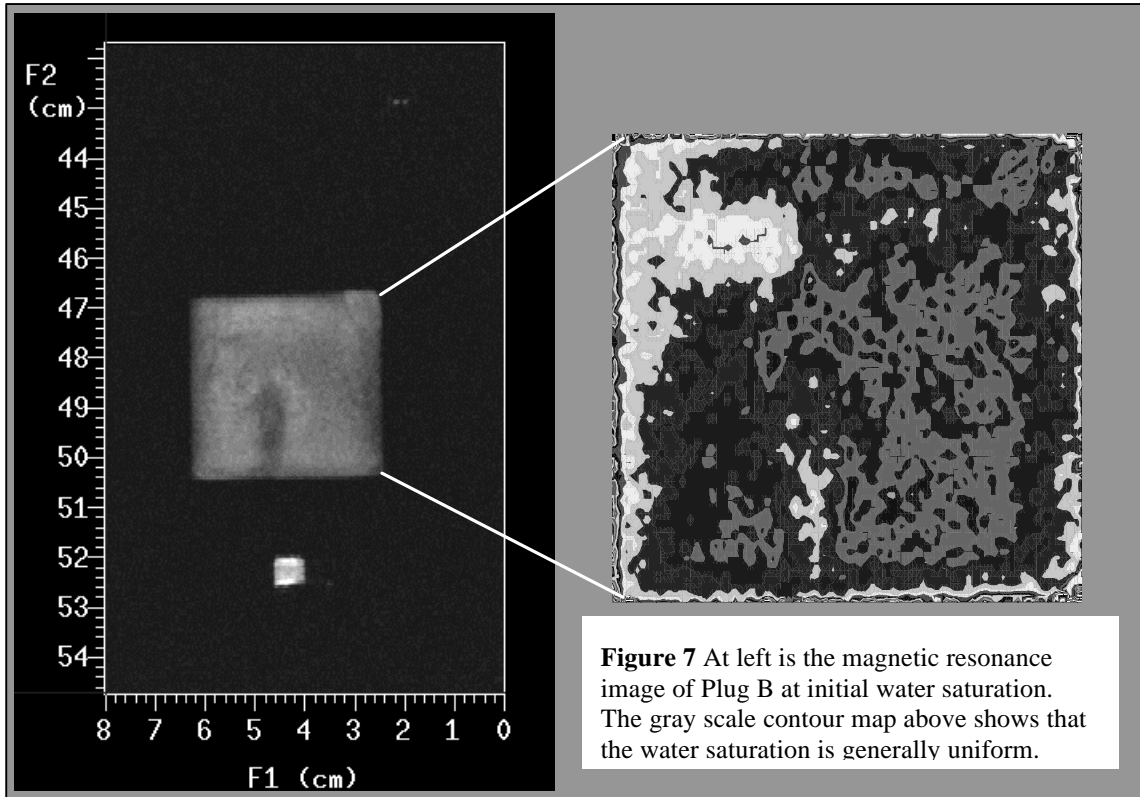


Figure 6 Results of the 3-D spontaneous imbibition test for plug B after aging to an apparent near-neutral wettability.



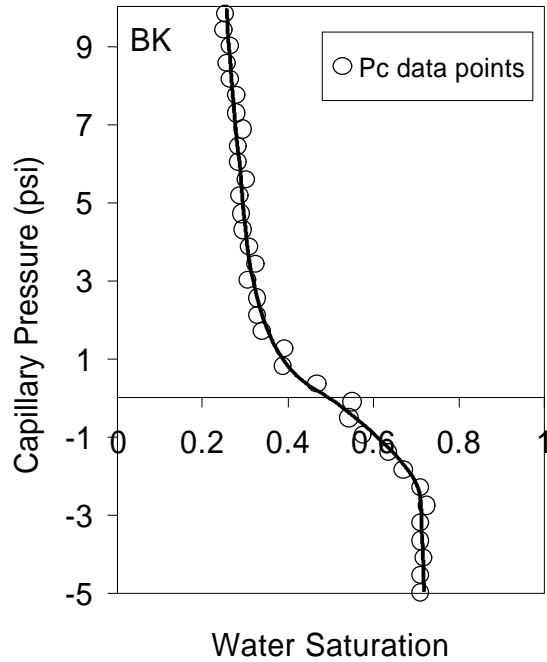


Figure 9a Imbibition Pc curve at position BK near the left edge within Plug B showing moderately water-wet behavior.

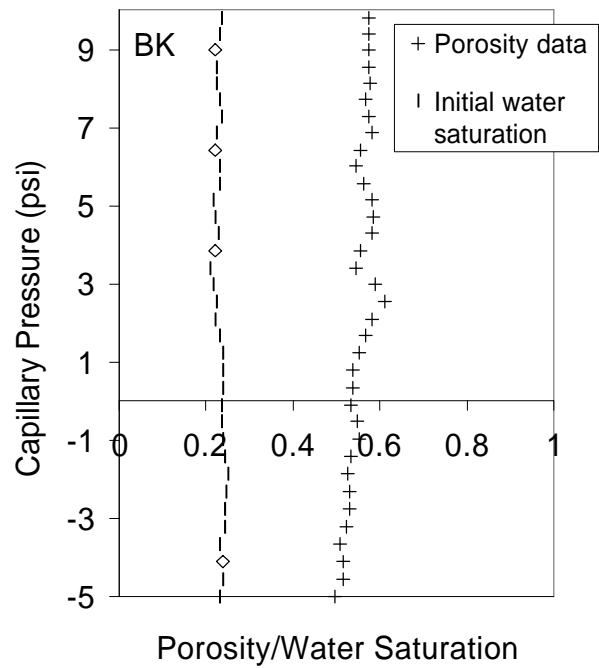


Figure 9b Porosity and initial water saturation values for Imbibition Pc curve at position BK near the left edge within Plug B.

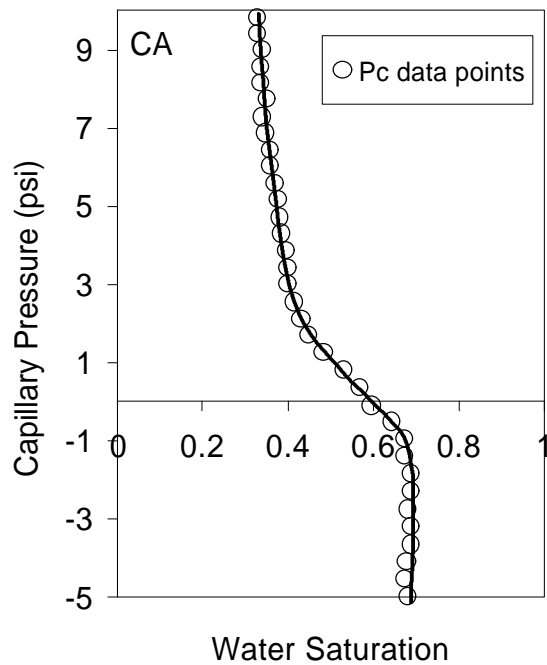


Figure 10a Imbibition Pc curve at position CA approximately midway from the left edge and center of Plug B showing water-wet behavior.

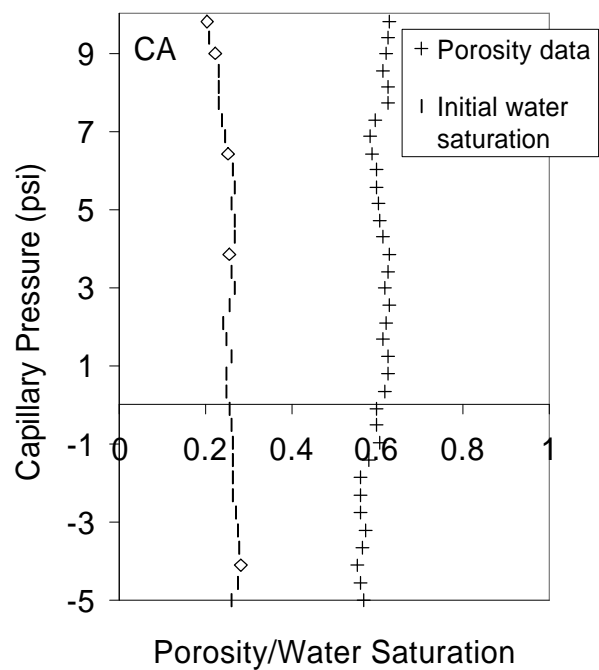


Figure 10b Porosity and initial water saturation values for Imbibition Pc curve at position CA approximately midway from the left edge and center of Plug B.

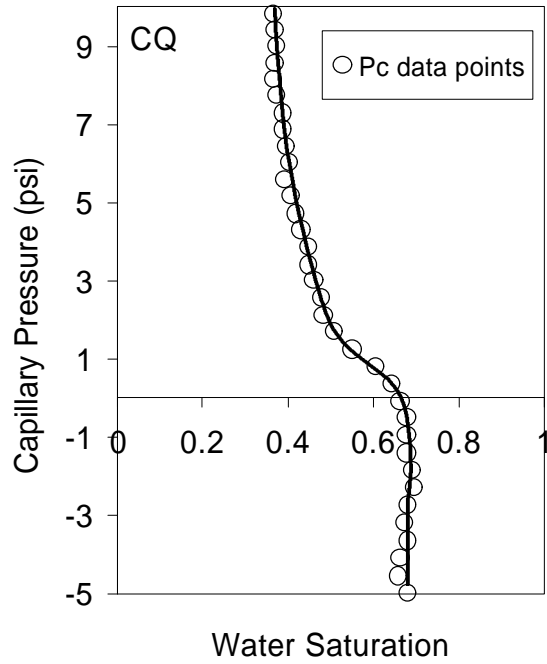


Figure 11a Imbibition Pc curve at position CQ left of the fracture within Plug B showing strongly water-wet behavior.

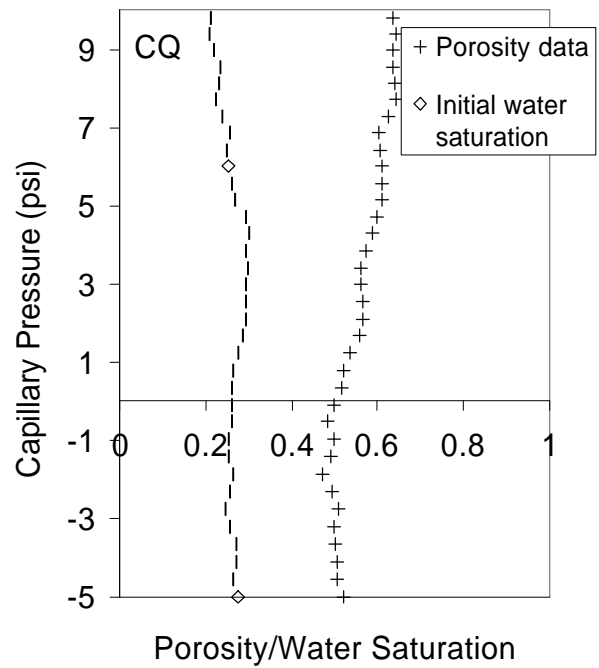


Figure 11b Porosity and initial water saturation values for Imbibition Pc curve at position CQ left of the fracture within Plug B.

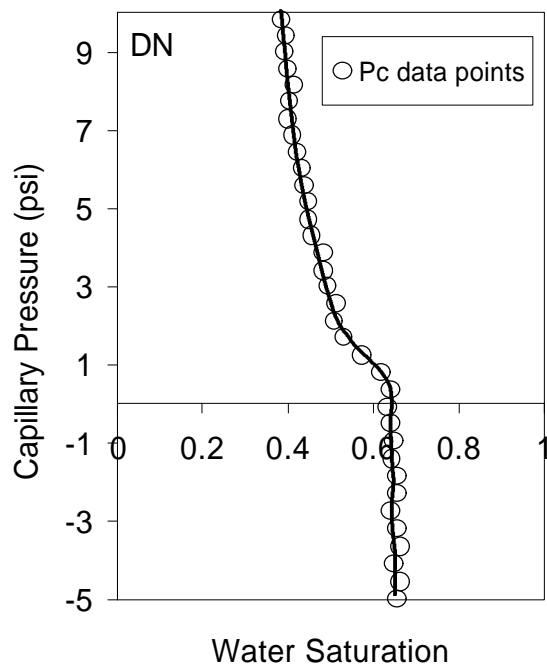


Figure 12a Imbibition Pc curve at position DN right of the fracture in Plug B near its center showing highly water-wet behavior.

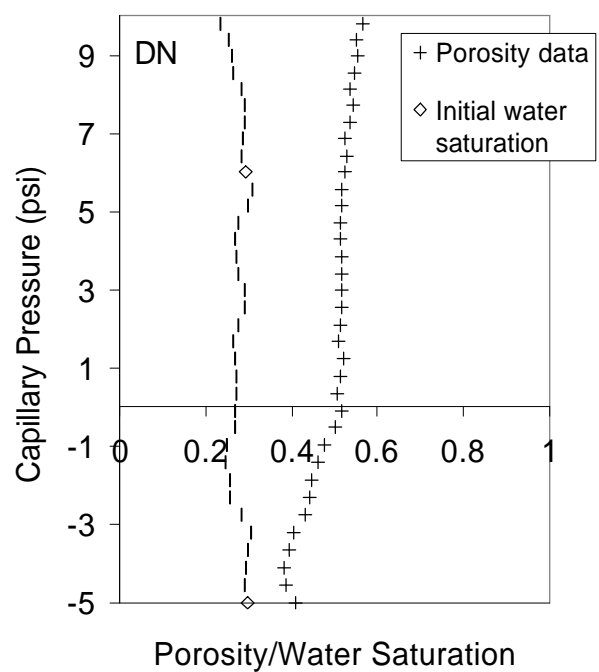


Figure 12b Porosity and initial water saturation values for Imbibition Pc curve at position DN right of the fracture in Plug B near its center.

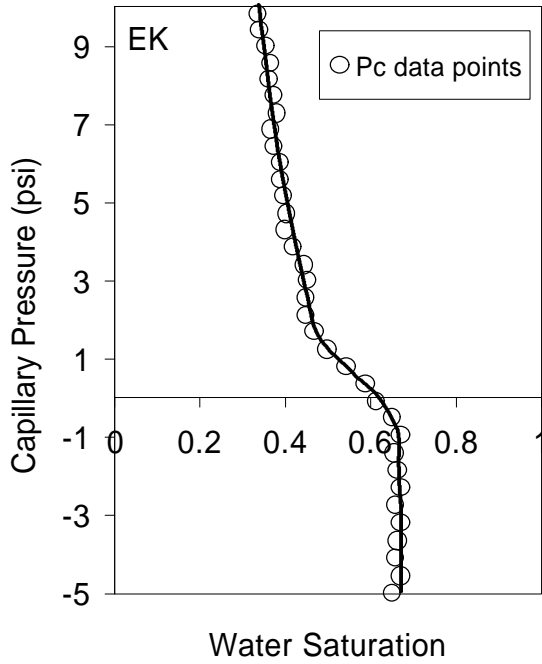


Figure 13a Imbibition Pc curve at position EK midway between center and the right edge of Plug B showing strongly water-wet behavior.

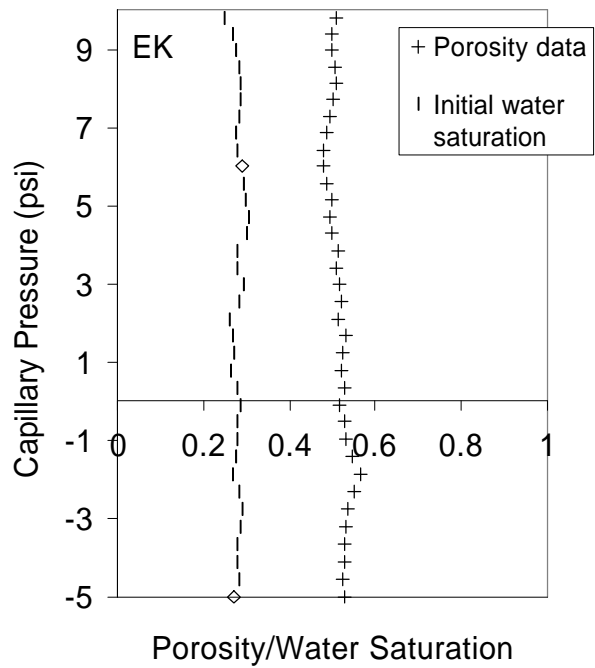


Figure 13b Porosity and initial water saturation values for Imbibition Pc curve at position EK midway between center and the right edge of Plug B.

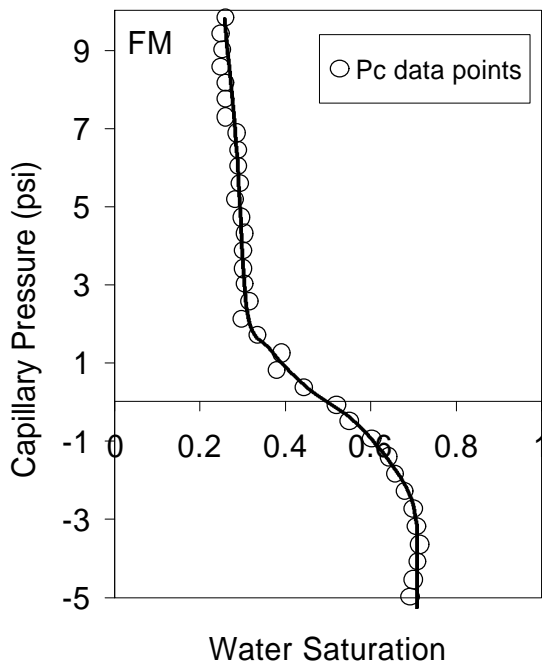


Figure 14a Imbibition Pc curve at position FM near the right edge within Plug B showing moderately water-wet behavior.

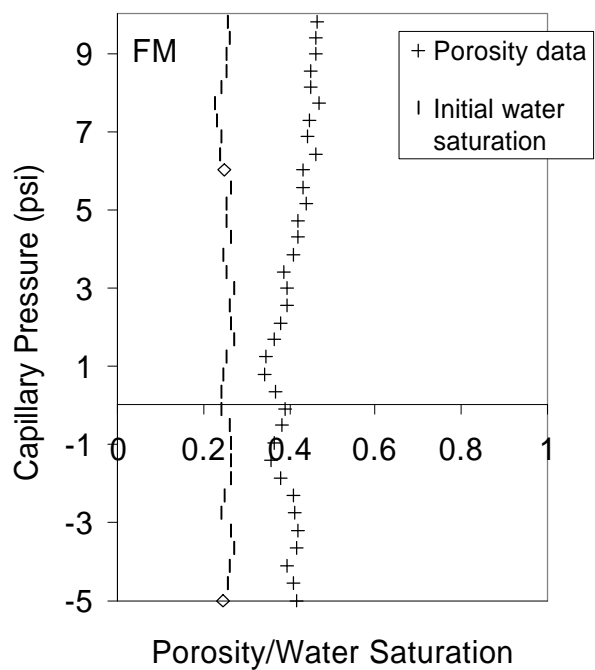


Figure 14b Porosity and initial water saturation values for Imbibition Pc curve at position FM near the right edge within Plug B.

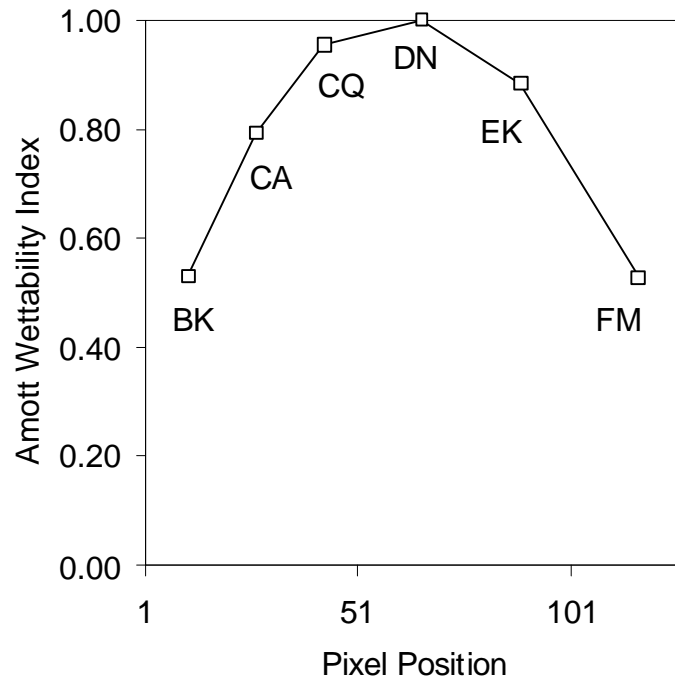


Figure 15 Amott wettability as a function of horizontal position within Plug B.

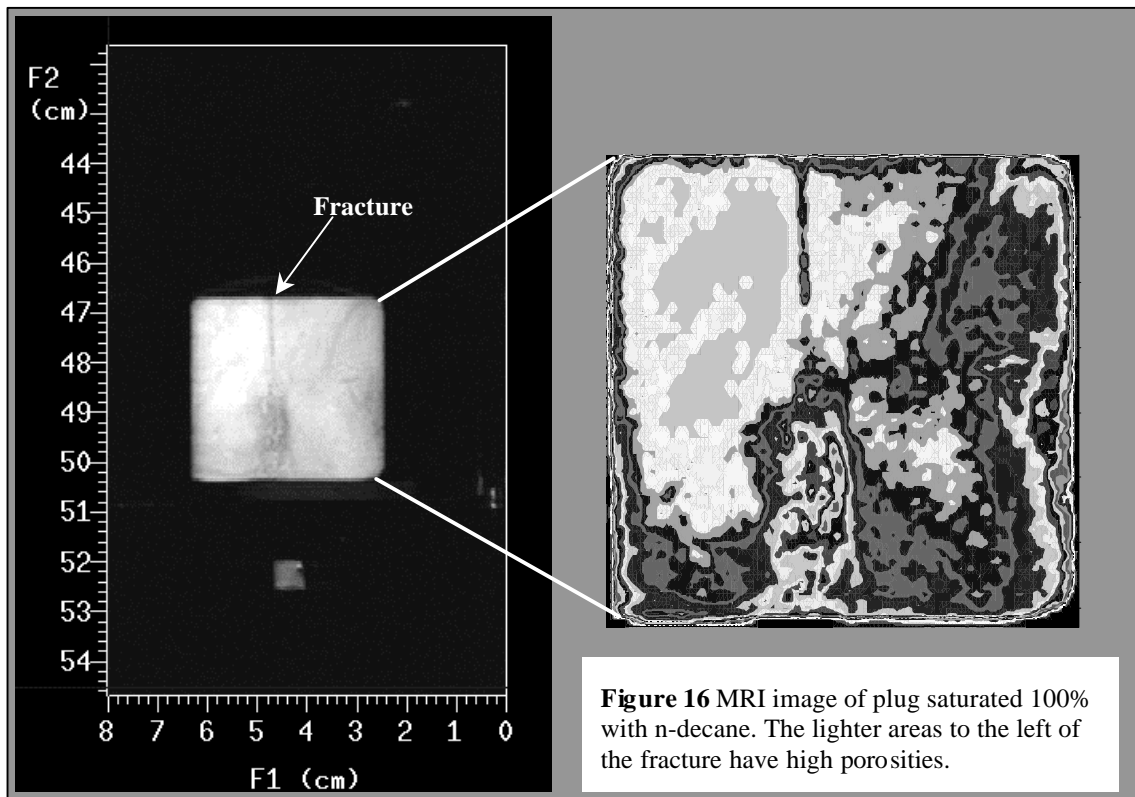


Figure 16 MRI image of plug saturated 100% with n-decane. The lighter areas to the left of the fracture have high porosities.